Mon. Not. R. astr. Soc. (1992) **255**, 119–128

W-modes: a new family of normal modes of pulsating relativistic stars

K. D. Kokkotas[1,2] and B. F. Schutz[2]

[1] *Section of Astrophysics, Astronomy and Mechanics, Department of Physics, University of Thessaloniki, Thessaloniki 540 06, Greece*

[2] *Department of Physics and Astronomy, University of Wales College of Cardiff, Cardiff CF1 3TH*

Accepted 1991 October 2. Received 1991 August 19

SUMMARY

We demonstrate explicitly the existence of a new family of outgoing-wave normal modes of pulsating relativistic stars, the first such family known that has *no analogue* in Newtonian stars. These modes were discovered earlier by the authors in a toy model, where they were called strongly damped normal modes. Kojima then found the first examples of these modes in realistic spherical polytropic stellar models. Here we give a number of arguments that demonstrate the existence of this family unequivocally, and we calculate a large number of eigenfrequencies. Physically, the modes arise directly from the coupling of the fluid oscillations of the star to the gravitational-wave oscillations of the space-time metric. Previously studied modes of relativistic stars have been close analogues of modes of Newtonian stars, where the coupling to gravitational waves mainly generates a small imaginary part to the frequency. Such modes can be classified using the Newtonian classes: *f*-, *p*-, *g*- and *r*-modes. The present modes, by contrast, have *no* Newtonian analogue. They are primarily oscillations of the space-time metric in which the fluid hardly vibrates at all. We christen them *w-modes* (gravitational-*w*ave *modes*). These modes are strongly damped, being characterized by complex frequencies with unusually large imaginary parts, comparable to their real parts. We calculate a sequence of $l=2$ modes for a number of spherical polytropic stellar models. An interesting feature of *w*-modes is that the lowest order mode of each sequence has a frequency similar to that of the lowest order mode of a spherical black hole. For higher modes, the spectrum diverges from the black-hole spectrum, but shows remarkable similarity to that of the strongly damped modes of the toy problem. As carriers of gravitational-wave information, *w*-modes may be important and observable in the burst of gravitational radiation that follows the formation of a neutron star. They should also be essential in solving the problem of the completeness of the outgoing-wave normal modes of radiating systems.

1 INTRODUCTION

The non-radial oscillations of neutron stars in general relativity, characterized by the emission of gravitational radiation, provide a unique probe of the coupling of strong gravitational fields to matter at supranuclear densities. The potential observability of such modes with future gravitational-wave detectors (Schutz 1989) or in X-ray observations makes it important to understand their spectrum fully. In addition, there are important unanswered mathematical questions that require a full understanding of the spectrum, such as the completeness of the normal modes for describing arbitrary initial perturbations of stars.

The equations which describe the non-radial pulsations of non-rotating relativistic stellar models were first found by Thorne & Campolattaro (1967a,b). They proved that Einstein's equations describing small, non-radial, even-parity, quasi-periodic oscillations of relativistic stellar models could be reduced to a fifth-order system of ordinary differential equations. Sixteen years later Lindblom & Detweiler (1983) reduced the system of the equations to a fourth-order one. This system is more natural, since from physical arguments one expects to have two second-order differential equations coupled together, the first describing the fluid perturbations and the second the gravitational-wave freedom. The fourth-order system seems to be irreducible, although very recent work by Chandrasekhar & Ferrari (1991a,b) has further simplified the form that the system takes. A detailed review of the work that was done before 1985 can be found in Kokkotas (1985).

When stellar oscillations couple with gravitational waves they are usually damped because the waves carry away the pulsational energy of the star. [There are circumstances where the loss of energy to gravitational radiation causes certain modes of rotating stars to grow (Chandrasekhar 1970; Friedman & Schutz 1978), but such instabilities are not of concern to us in this paper.] The eigenfrequencies of the normal modes of the system become complex; the real part gives the pulsation rate and the imaginary part the damping of the pulsation as a result of the emission of the gravitational radiation. In all previously studied modes, the imaginary part of the frequency was found to be very small compared to the real part, which leads to a slow decay of the oscillation. Kokkotas & Schutz (1986), studying a simple 'toy' radiating system, found a new family of normal modes of oscillations, in which the system rapidly loses energy: the eigenfrequencies have an imaginary part which is comparable to their real part. We conjectured there that realistic stars should exhibit these modes as well, and we prove that here.

Because the comparison of our results with those of the toy problem is important in establishing that we have indeed found this class of modes, we shall briefly describe the toy problem and its motivation. The physical system we wish to study – the relativistic star – can be thought of as two coupled dynamical systems. These are the fluid of which the star is made, and the gravitational field of general relativity, which has its own independent dynamical freedom. They are coupled, and the strength of the coupling depends on how relativistic the star is. The toy problem models the essentials of this system: it consists of two one-dimensional strings, coupled by a spring of spring constant k. One string is finite and tied down at both ends; it models the star, with its p-modes. The other string is semi-infinite, being tied down at one end. We place an outgoing-wave boundary condition at infinity on this string. This models the gravitational-wave field. The spring that connects the centre of the finite string to the semi-infinite one models the real coupling of gravitational waves to fluid motions.

If the coupling is weak, then the modes of the finite string are hardly disturbed by the coupling; the main effect is that they leak energy to the other string, which is then radiated away down it. This gives such modes a small imaginary part to their frequency. In the absence of coupling, the semi-infinite string does not have modes at all. The coupling does, however, create such modes. Since their energy is concentrated predominantly on the semi-infinite string, they radiate the energy away quickly, so they are strongly damped. If the coupling increases, then more of the energy is transferred to the finite string instead of being directly radiated away, and the damping is slower. As the coupling is weakened, the strongly damped eigenfrequencies move off to imaginary infinity in the complex frequency plane, where they disappear when the coupling is turned off completely.

Stimulated by the toy model, Kojima (1988) was the first to look for and find strongly damped modes in realistic polytropic stellar models. As we explain below, the problem is a delicate one numerically, and Kojima's method was best suited to weakly relativistic models. In this paper we give two alternative methods of finding the eigenfrequencies, which are better suited to the relativistic regime. Where we study some of Kojima's more relativistic models, our methods give eigenfrequencies that agree satisfactorily with each other, and which are not very different from those of Kojima. Because of the numerical delicacy, further work will be required before the spectrum of these modes is fully understood. Nevertheless, we feel that the present results are sufficient to establish without any doubt that the w-modes are indeed the strongly damped modes of the relativistic star.

The plan of the paper is as follows. In the next section we shall briefly discuss the theory of non-radial oscillations for relativistic stars and we shall write down the form of the equations that we shall use. In Section 3 we shall describe the two methods we adopt for solving the normal-mode equation; and in Section 4 we present and analyse our results. Finally in the last section we discuss the significance of the results.

2 THE PERTURBATION EQUATIONS

In this paper we follow Lindblom & Detweiler (1983; see also Detweiler & Lindblom 1985) in formulating the perturbation equations, which we briefly describe in this section.

The unperturbed metric is the general static spherically symmetric metric, which describes the geometry of an equilibrium stellar model:

$$ds^2 = -e^{\nu(r)}\,dt^2 + e^{\lambda(r)}\,dr^2 + r^2(d\theta^2 + \sin^2\theta\,d\phi^2), \tag{1}$$

with

$$e^{-\lambda(r)} = 1 - \frac{2M(r)}{r}, \tag{2}$$

where $M(r)$ is the 'gravitational mass' inside the radius r.

The hydrostatic equilibrium is described by the usual equations (*cf.* Schutz 1983):

$$\frac{dM}{dr} = 4\pi r^2 \rho, \tag{3}$$

$$\frac{d\nu}{dr} = 2\,\frac{(M + 4\pi r^3 p)}{r(r-2M)}, \tag{4}$$

$$\frac{dp}{dr} = -\frac{(\rho + p)}{2}\frac{d\nu}{dr}, \tag{5}$$

where ρ and p are the energy density and the pressure of the fluid inside the star. The pressure and density are related by an equation of state $\rho = \rho(p)$, which in this paper we take to be polytropic, i.e.,

$$p = K\rho^{1+(1/n)}, \tag{6}$$

where K and n are constants. The adiabatic index γ is given by:

$$\gamma = \frac{\rho + p}{p}\frac{dp}{d\rho}. \tag{7}$$

This equation of state was used by Balbinski *et al.* (1985) in their test of the quadrupole formula, and by Kojima (1988) in his search for strongly damped modes. We have chosen to use it rather than a more realistic one for two reasons: (i) our aim is to establish the existence of *w*-modes, and so we do not want to complicate the analysis with irrelevant details, and (ii) this allows us to compare our results for the *f*-modes with those of Balbinski *et al.* (1985) in order to test our numerical procedure.

The method of integrating the equilibrium equations for a specific model is standard (*cf.* Schutz 1983). The perturbations of the static spherical star can be decomposed into the appropriate spherical harmonics $Y_{\ell m}$ and are assumed to have a harmonic time dependence $e^{i\omega t}$. Then the perturbed metric can be written in Regge–Wheeler gauge in the following form:

$$ds^2 = -e^{\nu}(1 + r^{\ell} H_0 Y_{\ell m} e^{i\omega t})\, dt^2 - 2i\omega r^{\ell+1} H_1 Y_{\ell m} e^{i\omega t}\, dt\, dr + e^{\lambda}(1 - r^{\ell} H_0 Y_{\ell m} e^{i\omega t})\, dr^2 + r^2(1 - r^{\ell} K Y_{\ell m} e^{i\omega t})(d\theta^2 + \sin^2\theta\, d\phi^2). \quad (8)$$

The perturbation of the fluid inside the star is described by the Lagrangian displacement vector ξ^a with components:

$$\xi^r = r^{\ell-1} e^{-\lambda/2} W Y_{\ell m} e^{i\omega t}, \quad (9a)$$

$$\xi^\theta = -r^{\ell-2} V \frac{\partial}{\partial\theta} Y_{\ell m} e^{i\omega t}, \quad (9b)$$

$$\xi^\phi = -\frac{r^{\ell-2}}{\sin^2\theta} V \frac{\partial}{\partial\phi} Y_{\ell m} e^{i\omega t}. \quad (9c)$$

The five perturbation functions H_0, H_1, K, V and W depend only on r and are not all linearly independent; instead, the Einstein equations imply that they satisfy the following relation:

$$(2M + nr + Q)H_0 = +8\pi r^3 e^{-\nu/2} X - [(n+1)Q - \omega^2 r^3 e^{-(\lambda+\nu)}] H_1 + \left[nr - \omega^2 r^3 e^{-\nu} - \frac{e^{\lambda}}{r} Q(2M - r + Q) \right] K, \quad (10)$$

where

$$Q = M + 4\pi r^3 p, \qquad n = \tfrac{1}{2}(\ell+2)(\ell-1),$$

and the function X is defined by:

$$X = \omega^2(\rho + p) e^{-\nu/2} V - r^{-1} p' e^{(\nu-\lambda)/2} W + \tfrac{1}{2}(\rho + p) e^{\nu/2} H_0. \quad (11)$$

The Detweiler–Lindblom form of the equations is:

$$r e^{-\lambda} H_1' = -[(\ell+1) e^{-\lambda} + 2Mr^{-1} + 4\pi r^2 (p - \rho)] H_1 + H_0 + K - 16\pi(\rho + p) V, \quad (12a)$$

$$rK' = H_0 + (n+1) H_1 - \left[\ell + 1 - \frac{\nu' r}{2} \right] K - 8\pi(\rho + p) e^{\lambda/2} W, \quad (12b)$$

$$rW' = -(\ell+1) W + r^2 e^{\lambda/2} [(\gamma p)^{-1} e^{-\nu/2} X - \ell(\ell+1) r^{-2} V + \tfrac{1}{2} H_0 + K], \quad (12c)$$

$$rX' = -\ell X + \frac{1}{2}(\rho + p) e^{\nu/2} \left\{ \left(1 - \frac{\nu' r}{2}\right) H_0 + [r^2 \omega^2 e^{-\nu} + (n+1)] H_1 + \left(\frac{3}{2}\nu' r - 1\right) K - \ell(\ell+1) \nu' r^{-1} V - [8\pi(p + \rho) e^{\lambda/2} + 2\omega^2 e^{\lambda/2 - \nu} - r^2 (r^{-2} e^{-\lambda/2} \nu')'] W \right\}. \quad (12d)$$

If we regard H_0 in the right-hand side of these equations as the function of X, H_1 and K that is given in equation (10), then this system of four differential equations can be written in vectorial form as

$$\mathbf{Y}'(r) = \mathbf{Q}(r, \ell, \omega)\, \mathbf{Y}(r), \quad (13)$$

where $\mathbf{Y}$ is the vector

$$\mathbf{Y} = \{H_1, K, W, X\}, \quad (14)$$

while the 4×4 matrix $\mathbf{Q}$ depends on r, ℓ and ω.

The equations (12a–d) form a fourth-order system of linear differential equations. For every choice of ℓ and ω there will exist four linearly independent solutions. The physical solutions satisfy appropriate boundary conditions at the surface and the centre of the star. The perturbations must be finite at the centre of the star where the system becomes singular for $r=0$. At the surface of the star ($r=R$) the function $X(r)$ must vanish; this is equivalent to the vanishing of the perturbed pressure. These conditions in general allow only one physically acceptable solution to exist inside the star. When continued outside the star, this will consist in general of a mixture of incoming and outgoing radiation. A normal mode is defined as a solution for which there is pure outgoing radiation.

The complex value of ω for such a solution is its eigenfrequency. Such eigenfrequencies are generally located at discrete places in the complex-ω plane.

2.1 Numerical solution inside the star

Fixing ℓ and ω, we find the regular solution as follows. At the surface of the star, the boundary condition $X(R)=0$ allows us to select three linearly independent vectors $\mathbf{Y}_1$, $\mathbf{Y}_2$ and $\mathbf{Y}_3$ as initial data and to integrate them inwards from $r=R$ to $r=R/2$. The solution we seek will be a linear combination of these three solutions:

$$\mathbf{Y}_{\rm surf} = a_1 \mathbf{Y}_1 + a_2 \mathbf{Y}_2 + a_3 \mathbf{Y}_3. \quad (15)$$

We then start at the centre of the star with a Taylor approximation of the form

$$\mathbf{Y}(r) = \mathbf{Y}(0) + \tfrac{1}{2}\mathbf{Y}''(0) r^2. \quad (16)$$

The regularity conditions at the centre allow two linearly independent solutions $\mathbf{Y}_4$ and $\mathbf{Y}_5$. We integrate these from near $r=0$ to $r=R/2$. The solution we seek is a linear combination of the form:

$$\mathbf{Y}_{\rm cent} = a_4 \mathbf{Y}_4 + a_5 \mathbf{Y}_5. \quad (17)$$

Of the coefficients a_1, a_2, a_3, a_4, a_5 that we have introduced, one is an arbitrary linear scale. The other four are determined by matching the inner and outer solutions at $r=R/2$:

$$\mathbf{Y}_{\rm cent}(R/2) = \mathbf{Y}_{\rm surf}(R/2).$$

This determines the regular solution for the chosen ℓ and ω. Our procedure is essentially that of Lindblom & Detweiler (1983); for more detailed information one should refer to their paper. The main difference in the present paper is that we allow ω to be complex, which forces $\boldsymbol{Y}$ and the coefficients a_j to be complex as well. Another important difference is in the numerical procedure that we have used here for handling the static background star, i.e. the functions M, ν, p and ρ. Instead of calculating their values on a fixed grid of points and then using them in our calculations, we prefer to solve the system of equations (3)–(5) in parallel with the system (12) in order to adaptively refine the grid until we achieve a pre-determined accuracy.

2.2 The solution outside the star

In order to decompose the solution found in the previous section into incoming and outgoing waves, we must continue the numerical integration outside the star. The system of equations (12a–d) changes outside the star since there is no matter and the fluid perturbations vanish. The fourth-order system of differential equations reduces to a single-order differential equation, which, as was shown by Fackerell (1971), is Zerilli's (1970) one-dimensional wave equation

$$\frac{d^2 Z}{dr_*^2}+[\omega^2-V(r_*)]Z=0, \tag{18}$$

where $V(r_*)$ is the effective potential

$$V(r_*)=\frac{2(1-2M/r)}{r^3(nr+3M)^2}[n^2(n+1)r^3+3n^2Mr^2+9nM^2r+9M^3], \tag{19}$$

and r_* is the 'tortoise' coordinate, related to r by

$$r_*=r+2M\log(r-2M). \tag{20}$$

Equation (18) admits two linearly independent solutions that asymptotically represent outgoing and incoming waves; they admit the following asymptotic approximation near $r=\infty$:

$$Z_\pm=e^{\pm i\omega r_*}\sum_{k=0}^{\infty} Z_k^\pm r^{-k}. \tag{21}$$

The coefficients $Z_k^\pm$ can be determined from a five-term recurrence relation derived by Chandrasekhar & Detweiler (1975). If we define $Z_+(r)$ and $Z_-(r)$ to be the solutions of the Zerilli equation (18) that have the respective asymptotic approximations given in (21), then we see that $Z_+(r)$ is the incoming-wave solution, while the $Z_-(r)$ is the solution for outgoing gravitational radiation. Any solution of the Zerilli equation is a linear combination of $Z_+(r)$ and $Z_-(r)$.

When we consider how to perform this calculation numerically, it is easiest to start with a description of how one goes about searching for eigenfrequencies with small imaginary parts, such as those for the *f*-, *p*- and *g*-modes. For a given harmonic index ℓ, one chooses a complex value for ω and finds the unique solution which is valid inside the star, as above. The values of H_1 and K at the surface of the star determine (Fackerell 1971) the initial values $Z_{\rm star}$ and $Z'_{\rm star}$ for the numerical integration of the Zerilli equation outside the star. One starts the numerical integration of the Zerilli equation from $r=R$, producing the solution

$$Z_{\rm outside}(\omega,\ell;r)=A_\ell(\omega)Z_-(r)+B_\ell(\omega)Z_+(r), \tag{22}$$

outside the star. One continues this integration out to a radius large enough to give a clean separation between Z_+ and Z_-; we have found that $50|\omega|^{-1}$ is usually satisfactory. At this distance one matches the numerical values of Z and Z' to the corresponding values derived from the series solution (21). That is, one uses the numerical solution in the left-hand side of equation (22) and its derivative; one uses the asymptotic approximations (21) in the right-hand sides of these equations; and one solves the result for the coefficients $A_\ell(\omega)$ and $B_\ell(\omega)$. The eigenfrequency condition (no incoming radiation) is then

$$f_\ell(\omega)=\frac{B_\ell(\omega)}{A_\ell(\omega)}=0. \tag{23}$$

It is preferable to use the ratio $f(\omega)$ because it is independent of how the arbitrary scale factor in the set of coefficients a_j for the interior solution was chosen. The whole procedure may be viewed as solving the non-linear complex equation (23). This equation can be solved with Muller's iterative search technique (Press *et al.* 1986) using a parabolic approximation to the solution. One makes three initial guesses for the eigenfrequency and fits the resultant values of $f(\omega)$ to a parabola. The roots of this parabola will give a first approximate value for a complex root of $f(\omega)$. The procedure can be continued iteratively until a root is found to the desired accuracy. This can be repeated over the whole complex ω-plane if the complete spectrum is needed.

The numerical procedure that we have just described for integrating the Zerilli equation outwards gives good results when one searches in the complex ω-plane for frequencies with small imaginary part. For the *f*-, *p*- and *g*-modes, it is usually the case that $\mathrm{Im}(\omega)$ is at least 1000 times less than $\mathrm{Re}(\omega)$, and all searches for them have used some variant of this method. But if instead one searches the complex ω-plane for normal-mode frequencies with large imaginary parts, as we do here, this procedure runs into a well-known numerical difficulty. The two linearly independent solutions $Z_\pm(r)$ diverge rapidly in magnitude as $r\to\infty$ if the complex frequency has a large imaginary part, one of them increasing exponentially and the other decreasing exponentially. If we write

$$\omega=\sigma+i\tau, \tag{24}$$

then a stable star will have modes that damp, which implies $\tau>0$. In this case, equation (22) shows that the two solutions have the asymptotic behaviour

$$|Z_-|\sim e^{\tau r_*} \text{ and } |Z_+|\sim e^{-\tau r_*}. \tag{25}$$

When integrating outwards from $r=R$ to $r\to\infty$ the outgoing solution Z_- dominates over Z_+, and the extraction of Z_+, from a numerical solution of finite precision at a distance large enough for the asymptotic forms of $Z_\pm$ to be valid, becomes impossible. Any attempt to follow numerically the exponentially decreasing solution will always fail because the increasing one will dominate in the numerical calculations.

In the next section we describe the two different approaches that we use to avoid this numerical difficulty.

3 SOLVING THE ZERILLI EQUATION FOR LARGE DAMPING

We describe here the two methods we have used to avoid the difficulty we have just described for integrating the Zerilli equation when the imaginary part of the frequency is large. Both avoid integrating $Z_\pm$ numerically far from the star by performing the match between $Z_{\rm star}$ and $Z_\pm$ at the surface of the star.

3.1 The full WKB method

We cannot use the asymptotic approximation (21) to give us $Z_\pm$ at the surface of the star because it is valid only near infinity. Instead, we use the WKB solutions, which are different asymptotic approximations to $Z_\pm$ that should be good even at small r provided $|\omega|$ is large enough. The WKB approximation for the Zerilli equation (18) outside the star has the standard form:

$$Z(\omega,\ell;r_*)=Q(r_*)^{1/2}\left\{A_\ell(\omega)\exp\left[-i\int^{r_*}Q(x)\,dx\right]+B_\ell(\omega)\exp\left[i\int^{r_*}Q(x)\,dx\right]\right\},\qquad(26)$$

where

$Q(r_*)=[\omega^2-V(r_*)]^{1/2}.$

The coefficients $A_\ell(\omega)$ and $B_\ell(\omega)$ are the same as in equation (22) above. If we assume that this solution is a good approximation for $r>R$, then we need only match the solution (26) and its derivative at the surface of the star with the values $Z_{\rm star}(R)$ and $Z'_{\rm star}(R)$ found from the integration inside the star. Because of the arbitrary linear scale, we need only match the ratio

$$\frac{Z'_{\rm star}(\omega,\ell;R)}{Z_{\rm star}(\omega,\ell;R)}=\frac{A_\ell(\omega)Z'_-(R)+B_\ell(\omega)Z'_+(R)}{A_\ell(\omega)Z_-(R)+B_\ell(\omega)Z_+(R)},\qquad(27)$$

where the prime denotes derivation with respect to r_*. From this we calculate the same function as in equation (23):

$$f_\ell(\omega)=\frac{B_\ell(\omega)}{A_\ell(\omega)}=\exp[-2iQ(R)]\,\frac{Q(R)-i\left[\dfrac{Z'_{\rm star}(R)}{Z_{\rm star}(R)}+\dfrac{Q'(R)}{2Q(R)}\right]}{Q(R)+i\left[\dfrac{Z'_{\rm star}(R)}{Z_{\rm star}(R)}+\dfrac{Q'(R)}{2Q(R)}\right]}.\qquad(28)$$

It is more convenient to use the form

$$f(\omega)=\frac{B_\ell(\omega)}{A_\ell(\omega)}=\exp[-2iQ(R)]\times\frac{Q^2(R)-\left[\dfrac{Z'_{\rm star}(R)}{Z_{\rm star}(R)}+\dfrac{Q'(R)}{2Q(R)}\right]^2}{\left\{Q(R)+i\left[\dfrac{Z'_{\rm star}(R)}{Z_{\rm star}(R)}+\dfrac{Q'(R)}{2Q(R)}\right]\right\}^2}.\qquad(29)$$

in order to avoid calculating the root of a complex function. The eigenfrequencies ω can be found by calculating the zeros of $f(\omega)$ using the Muller method that we mentioned earlier.

How good should this method be? The WKB technique is widely used for solving problems that here correspond to real frequencies, when ω is large. It can, however, be applied in problems where ω is complex, and has notably been done so recently in searches for black-hole normal modes (Schutz & Will 1985; Guinn *et al.* 1990). The fundamental assumption of the technique, namely that the background potential $V(r_*)$ should vary slowly on the characteristic length-scale of the solution, $|\omega|^{-1}$, seems to be satisfied even when ω is complex. We expect errors, of course, if $M\omega\sim1$, but not uncontrollable errors; and these should decrease as $|\omega|$ increases. We use the second method, to which we now turn, partly in order to quantify these errors.

3.2 The mixed numerical/WKB method

As we have explained earlier the numerical procedure for solving the Zerilli equation when $\mathrm{Im}(\omega)$ is large breaks down. On the other hand, the fully analytic WKB approximation might not be very good if $|\omega|$ is not very large. An alternative is suggested by the following considerations. The numerical problem that we want to get around is that only one of the two desired solutions $Z_\pm$ can be found numerically: as equation (25) shows, if one integrates outwards from the surface (with, say, roughly equal initial values for the two functions) one finds Z_- accurately far away, but Z_+ disappears in the roundoff error; while if one integrates inwards from a large radius, one finds Z_+ accurately at the surface, but Z_- disappears. The full WKB method replaces *both* functions by their WKB approximations; our second variant will be to calculate one of them accurately numerically, and essentially to replace only the missing one with the WKB function. While this still suffers from WKB errors, a comparison of its results with those from the first method should serve to quantify the size of these errors.

Since we need to start our external solution from initial data at the surface, we choose to calculate the incoming solution Z_+ accurately from a numerical integration that starts far away. It is not hard to choose the starting values for Z_+ and Z'_+ far away, since any admixture of Z_- in the solution will disappear by the time we reach the surface of the star. We use the series solution (21), but one could equally well use a WKB approximate solution far away to start off.

The ratio we want is, in this case,

$$f_\ell(\omega)=\frac{B_\ell(\omega)}{A_\ell(\omega)}=\frac{Z'_-(R)/Z_-(R)-Z'_{\rm star}/Z_{\rm star}}{Z_-(R)[Z_+(R)Z'_{\rm star}/Z_{\rm star}-Z'_+(R)]}.$$

Zeros of this are the same as zeros of the simpler function

$$g_\ell(\omega)=\frac{Z'_{\rm star}}{Z_{\rm star}}-\frac{Z'_-(R)}{Z_-(R)}.\qquad(30)$$

To calculate this, it is not necessary to use the full form of the WKB approximation for the second solution Z_-. All we need is the ratio $Z'_-(R)/Z_-(R)$, and this is easy to find from the numerical values for $Z'_+(R)/Z_+(R)$, since within the WKB approximation we have

$$\frac{Z'_-}{Z_-}=-\frac{Z'_+}{Z_+}-\frac{Q'(R)}{Q(R)},\qquad(31)$$

where $Q=[\omega^2-V(r_*)]^{1/2}$, and the prime denotes derivation with respect to r_*. The proof of this comes from considering the WKB logarithmic derivatives

$$\frac{Z_+'}{Z_+}=iQ-\frac{Q'}{2Q} \tag{32a}$$

and

$$\frac{Z_-'}{Z_-}=-iQ-\frac{Q'}{2Q}, \tag{32b}$$

from which (31) can easily be deduced.

Although this method still relies on the WKB assumptions, it uses them in a way significantly different from that of the first method. We expect, therefore, that the errors made by the two methods will be comparable but different: the difference between the two methods should give a measure of the error in each.

4 RESULTS

We have applied the numerical methods just described to a few stellar models with the polytropic equation of state (6). We took the constants n and K to have the values $n=1$ and $K=100$ km. The models are then characterized by their central density. We have constructed a complete family, from weakly relativistic models (central density 3×10^{14} g cm^{-3}, surface redshift 0.081) up to the ultrarelativistic regime (3×10^{16} g cm^{-3}, 0.623). As a test, for each model we calculated the fundamental *f*-mode frequency by the method of Section 2 and compared it with the existing results from Balbinski *et al.* (1985) in order to check that the equations inside the star give the correct results. Then we tested the full WKB method (Section 3.1) by calculating the *f*-mode frequency. The agreement was usually very good for the real part of the frequency (the difference was of the order less than 1 per cent). The accuracy for the imaginary part was worse – it usually came out a factor of 10 or more too small – but we should not be surprised at this since Im(ω) is a tiny fraction of Re(ω). We then used the two methods described in Section 3 to search for normal-mode frequencies in the complex plane well away from the real axis.

The results that we have found are remarkable. A well-defined spectrum of normal-mode frequencies does indeed exist, with frequencies whose large imaginary parts are comparable to their real parts. A striking feature is that, as the order of the mode increases, the real parts of the frequencies increase with a nearly constant step while the imaginary parts vary only slowly. These frequencies are shown in Tables 1, 2, 3 and 4 for four stellar models.

Their values are plotted in Fig. 1, where we also include the normal-mode frequencies of a Schwarzschild black hole. This shows three interesting features. The first is that the spectrum starts from frequencies which are very close to those of a black hole of similar mass. The nature of this relationship between stellar normal modes and those of black holes is not yet clear, but since this class of stellar modes is dominated by metric perturbations rather than fluid disturbances, some sort of relationship is not surprising. The different boundary conditions for the stellar and black-hole problems, however, prevent one making any simple connection.

Table 1. (a) Full WKB method and (b) numerical WKB method.

(a)

N	Re(ωM)	Δ Re(ω)	Im(ωM)	Re(ω)	Δ Re(ω)	Im(ω)
1	.3350		.4060	.2833		.3430
2	.5960	(.26)	.3560	.5039	(.22)	.3006
3	.8898	(.29)	.3850	.7518	(.25)	.3253
4	1.1632	(.27)	.4123	.9827	(.23)	.3484
5	1.4332	(.27)	.4509	1.2109	(.23)	.3810
6	1.6997	(.27)	.4651	1.4361	(.23)	.3930
7	1.9409	(.24)	.4808	1.6398	(.20)	.4062
8	2.1537	(.21)	.5083	1.8196	(.18)	.4295

(b)

N	Re(ωM)	Δ Re(ω)	Im(ωM)	Re(ω)	Δ Re(ω)	Im(ω)
1	.3419		.1770	.2884		.1496
2	.6489	(.31)	.2423	.5482	(.26)	.2047
3	.9236	(.27)	.2830	.7803	(.23)	.2391
4	1.1919	(.27)	.3131	1.0060	(.23)	.2645
5	1.4575	(.27)	.3379	1.2314	(.23)	.2855
6	1.7211	(.26)	.3579	1.4541	(.22)	.3024
7	1.9676	(.25)	.3793	1.6623	(.21)	.3205
8	2.2370	(.27)	.4013	1.8900	(.23)	.3391
9	2.4590	(.22)	.4258	2.0776	(.19)	.3598

Table 2. (a) Full WKB method and (b) numerical WKB method.

(a)

N	Re(ωM)	Δ Re(ω)	Im(ωM)	Re(ω)	Δ Re(ω)	Im(ω)
1	.5280		.2980	.2822		.1595
2	.8780	(.35)	.3760	.4694	(.19)	.2013
3	1.2240	(.35)	.4280	.6547	(.19)	.2289
4	1.5685	(.35)	.4669	.8388	(.18)	.2497
5	1.9120	(.34)	.4980	1.0225	(.18)	.2662
6	2.2540	(.34)	.5240	1.2055	(.18)	.2804
7	2.5954	(.34)	.5435	1.3880	(.18)	.2907
8	2.9402	(.34)	.5575	1.5724	(.18)	.2981
9	3.2874	(.35)	.5526	1.7581	(.19)	.2956
10	3.7002	(.41)	.5411	1.9789	(.22)	.2894
11	4.0774	(.38)	.6043	2.1806	(.20)	.3232

(b)

N	Re(ωM)	Δ Re(ω)	Im(ωM)	Re(ω)	Δ Re(ω)	Im(ω)
1	.5154		.2581	.2756		.1380
2	.8757	(.36)	.3414	.4683	(.19)	.1826
3	1.2234	(.35)	.4949	.6543	(.19)	.2112
4	1.5674	(.34)	.4344	.8383	(.18)	.2323
5	1.9106	(.34)	.4653	1.0218	(.18)	.2488
6	2.2531	(.34)	.4912	1.2050	(.18)	.2627
7	2.5973	(.34)	.5123	1.3890	(.18)	.2740
8	2.9383	(.34)	.5233	1.5714	(.18)	.2799
9	3.2844	(.35)	.5196	1.7565	(.19)	.2779
10	3.7034	(.42)	.5063	1.9806	(.22)	.2707
11	4.0680	(.36)	.5841	2.1755	(.19)	.3124

The second interesting feature of Fig. 1 is that, generally, the less relativistic the model is, the larger is the damping rate of any mode. This was also seen in the toy problem of Kokkotas & Schutz (1986): as the coupling weakened, the damping increased.

Table 3. (a) Full WKB method and (b) numerical WKB method.

(a)

N	Re(ωM)	Δ Re(ω)	Im(ωM)	Re(ω)	Δ Re(ω)	Im(ω)
1	.5180		.1740	.2599		.0870
2	.8110	(.29)	.2690	.4069	(.15)	.1351
3	1.1040	(.29)	.3240	.5536	(.15)	.1626
4	1.4000	(.30)	.3630	.7022	(.15)	.1822
5	1.6937	(.29)	.3920	.8493	(.15)	.1967
6	1.9940	(.30)	.4140	.9999	(.15)	.2008
7	2.2867	(.29)	.4293	1.1466	(.15)	.2153
8	2.6011	(.31)	.4229	1.3043	(.16)	.2120
9	2.9545	(.35)	.4338	1.4814	(.18)	.2175
10	3.2864	(.33)	.4880	1.6479	(.17)	.2447

(b)

N	Re(ωM)	Δ Re(ω)	Im(ωM)	Re(ω)	Δ Re(ω)	Im(ω)
1	.5223		.1897	.2619		.0951
2	.8123	(.29)	.2889	.4073	(.15)	.1449
3	1.1016	(.29)	.3429	.5524	(.15)	.1719
4	1.3966	(.29)	.3800	.7003	(.15)	.1906
5	1.6893	(.29)	.4077	.8471	(.15)	.2044
6	2.9910	(.30)	.4292	.9984	(.15)	.2152
7	2.2831	(.29)	.4439	1.1448	(.15)	.2226
8	2.5999	(.32)	.4349	1.3036	(.16)	.2181
9	2.9478	(.35)	.4455	1.4781	(.17)	.2234
10	3.2848	(.34)	.5005	1.6471	(.17)	.2509
11	3.5735	(.29)	.5340	1.7926	(.15)	.2678

Table 4. (a) Full WKB method and (b) numerical WKB method.

(a)

N	Re(ωM)	Δ Re(ω)	Im(ωM)	Re(ω)	Δ Re(ω)	Im(ω)
1	.4620		.0800	.2409		.0415
2	.6825	(.22)	.1710	.3556	(.11)	.0891
3	.9100	(.23)	.2220	.4743	(.12)	.1158
4	1.1421	(.23)	.2566	.5950	(.12)	.1337
5	1.3750	(.23)	.2830	.7163	(.12)	.1472
6	1.6100	(.23)	.2974	.8387	(.12)	.1549
7	1.8522	(.24)	.3015	.9649	(.13)	.1571
8	2.1473	(.29)	.3068	1.1186	(.15)	.1598
9	2.3978	(.25)	.3506	1.2491	(.13)	.1858
10	2.6405	(.24)	.3784	1.3756	(.13)	.1971
11	2.8956	(.25)	.4000	1.5084	(.13)	.2084
12	3.1418	(.25)	.4148	1.6367	(.13)	.2161
13	3.4041	(.26)	.4263	1.7734	(.14)	.2221

(b)

N	Re(ωM)	Δ Re(ω)	Im(ωM)	Re(ω)	Δ Re(ω)	Im(ω)
1	.4632		.1033	.2413		.0538
2	.6838	(.22)	.1961	.3562	(.11)	.1022
3	.9074	(.22)	.2474	.4727	(.12)	.1289
4	1.1365	(.23)	.2795	.5921	(.12)	.1456
5	1.3685	(.23)	.3036	.7129	(.12)	.1581
6	1.6037	(.24)	.3166	.8354	(.12)	.1650
7	1.8477	(.24)	.3211	.9625	(.13)	.1673
8	2.1366	(.29)	.3232	1.1130	(.15)	.1684
9	2.3913	(.24)	.3728	1.2457	(.13)	.1942
10	2.6354	(.25)	.3938	1.3729	(.13)	.2052
11	2.8903	(.25)	.4134	1.5057	(.13)	.2153
12	3.1255	(.24)	.4288	1.6282	(.12)	.2234
13	3.3955	(.27)	.4445	1.7669	(.14)	.2315

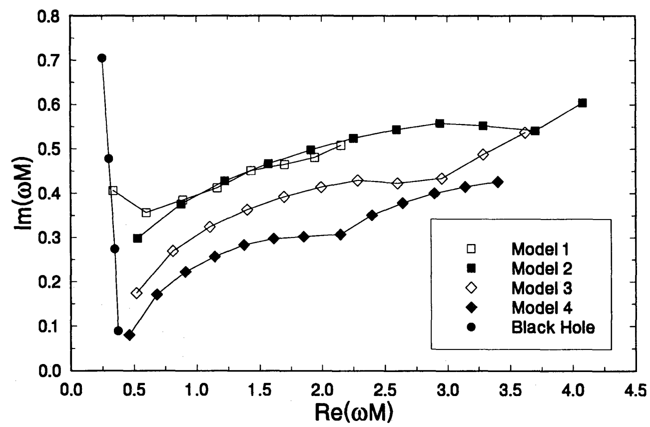

Figure 1. The frequency spectrum of w-modes for $\ell=2$ for four polytropic stellar models, calculated by the full WKB method, are plotted together with the spectrum of the Schwarzschild black-hole frequencies. All frequencies are made dimensionless by multiplication by the mass of the star. Note the proximity of the lowest w-mode of each model to the black-hole spectrum.

The third feature is the kink in each w-mode curve as the order of the mode increases. We have no explanation of this.

In Figs 2–5 we compare the eigenfrequencies of the four models as calculated by the two methods of Section 3. The agreement of the two methods is apparent and this means that any errors in the values of the eigenfrequencies due to the WKB approximation do not affect our confidence that we have in fact demonstrated the existence of this new family of modes.

In Fig. 6, we plot the frequencies in units of km^{-1}, i.e. not normalized by the stellar mass. The trend of stronger damping with weaker coupling is even more evident here than in Fig. 1.

We have plotted the eigenfrequencies that Kojima found together with ours in Figs 2 and 3. Some of his eigenfrequencies appear to be within our errors, but others are further away. Agreement is better for the more weakly relativistic star in Fig. 2, where Kojima's method is better and ours seems to be worse. In Fig. 3, Kojima's method is near its limits of validity, and his values are presumably not as reliable as ours.

Further evidence for the identification of our eigenfrequencies as strongly damped modes comes from an examination of the eigenfunctions. In Fig. 7 we compare the behaviour of the eigenfunctions for the metric perturbations K and H_1 for an f-mode and w-mode in Model 2. For both modes the eigenfunctions have been normalized to 1 at the surface ($r=8.861$ km). We display their values only within the star. It is clear that with this normalization, these metric perturbations have similar size throughout the star. Notice, however, that K and H_1 are in phase with each other for the w-mode, but out of phase for the f-mode.

The behaviour of the fluid perturbation W in the two modes is completely different (Fig. 8). With the normalization still fixed as in Fig. 7, the fluid perturbation inside the star is an order of magnitude smaller for the w-mode than for the f-mode. This is exactly what one expects from our interpretation of the w-mode, and exactly what we see in the toy model. This disparity is not seen in any of the families of modes explored before this.

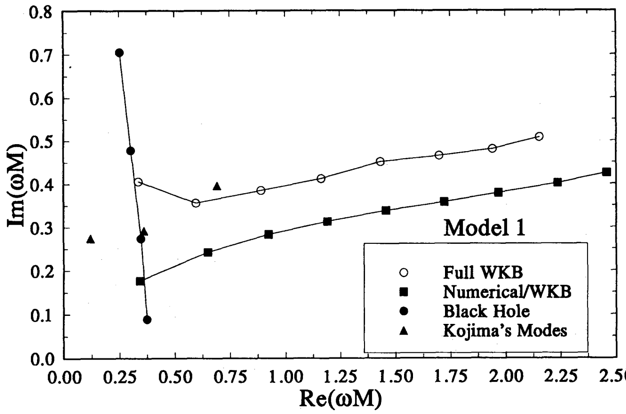

Figure 2. The $\ell=2$ *w*-mode spectrum of Model 1 (the least relativistic model). The characteristics of Model 1 may be found in the caption to Table 1. We give the results of both numerical methods described in the text, together with those for a Schwarzschild black hole. Agreement between the two methods is poorer than in the more relativistic models (later figures). The difference between the two is a measure of the accuracy of our determination of the eigenfrequencies. We show the three eigenfrequencies found by Kojima (1988) for the same model. These seem to be within our errors.

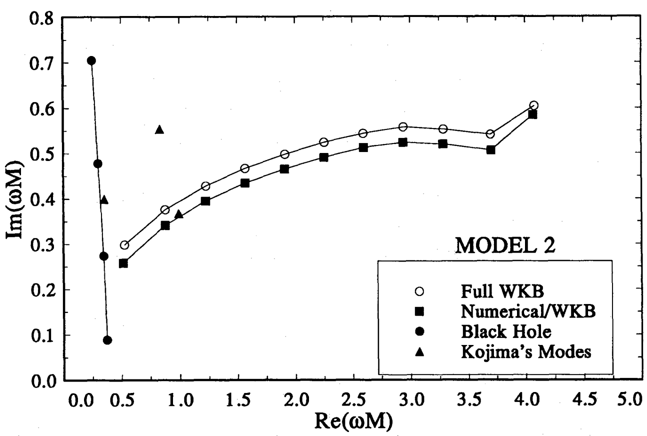

Figure 3. As Fig. 2 for Model 2. The characteristics of Model 2 may be found in the caption to Table 2. Agreement between the methods is much better than for Model 1. We show the three eigenfrequencies found by Kojima (1988) for this model. His values are rather far from ours, probably because his method is close to its limit of convergence for this model.

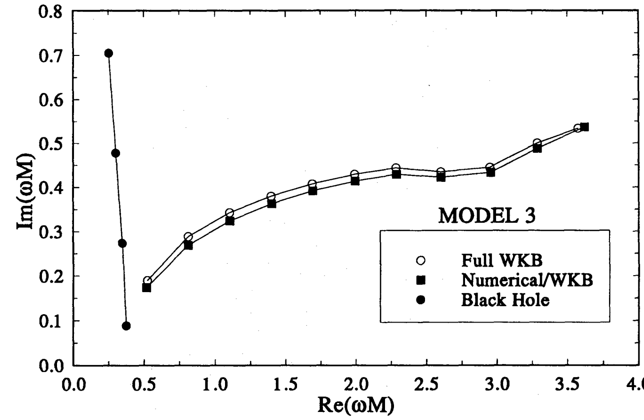

Figure 4. As Fig. 2 for Model 3. The characteristics of Model 3 may be found in the caption to Table 3. Our methods agree even better here.

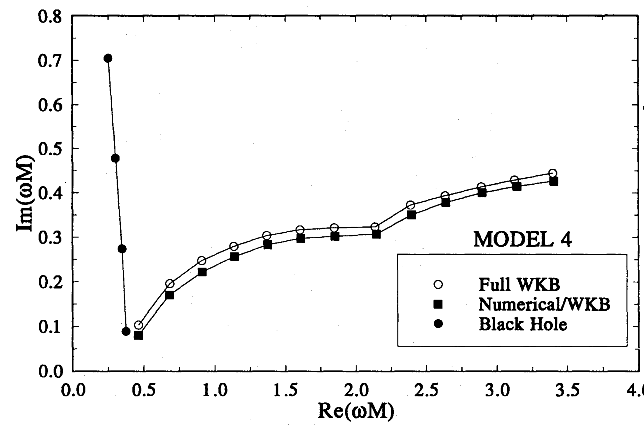

Figure 5. As Fig. 2 for Model 4. The characteristics of Model 4 may be found in the caption to Table 4. The errors have become very small in this highly relativistic model.

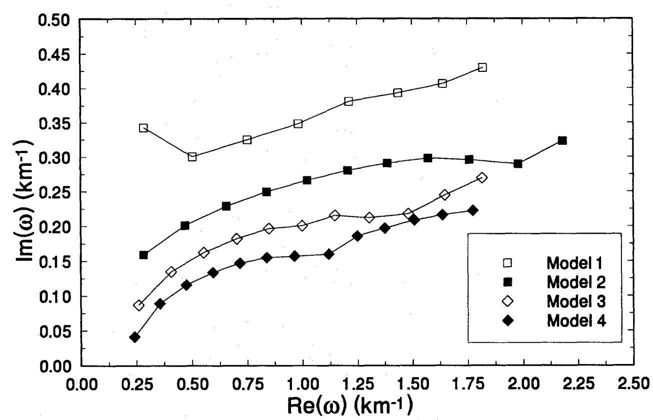

Figure 6. The frequency spectrum of $\ell=2$ *w*-modes for the four polytropic stellar models are plotted in units of km^{-1}. This shows the trend with increasing redshift very well.

5 DISCUSSION

We believe that these calculations convincingly establish that realistic stellar models do indeed have families of strongly damped normal modes in close analogy to those that we discovered in the toy problem, despite the numerical difficulty of finding them. There are a number of reasons, outlined below.

(i) In the toy model, the strongly damped sequence of eigenfrequencies had the property that the real part of the frequency increased in regular steps while the imaginary part remained essentially fixed; the imaginary part depended only on the coupling constant k, and was essentially logarithmic in it. In our case, the real part increases in regular steps, and the imaginary part increases only slowly. This increase in the imaginary part along the sequence is not necessarily in contradiction to the toy problem. In the toy problem, the

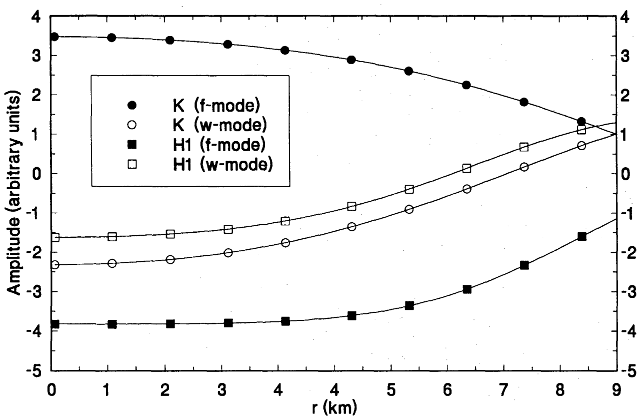

Figure 7. Comparison of the *metric perturbation* eigenfunctions (K and H_1) of a strongly damped w-mode (open symbols) with those of a weakly damped f-mode (filled symbols). The w-mode is the 'fundamental' of Model 2 from Fig. 2. The normalization is fixed by requiring $K=1$ at the surface. The plot covers the interior of the star only. With this normalization, there is little difference between the two modes' gravitational-wave amplitudes inside the star. This is in contrast to the fluid perturbation (Fig. 8).

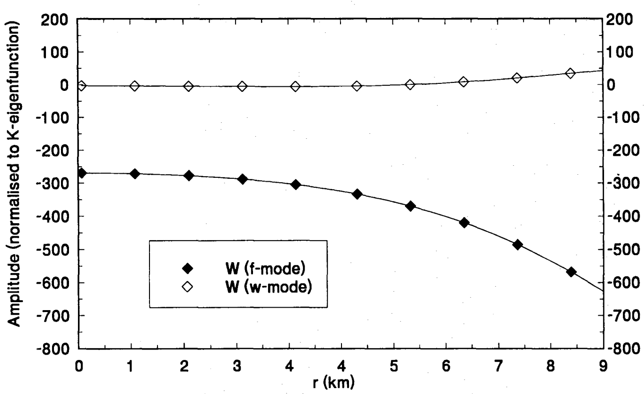

Figure 8. As Fig. 7, but for the eigenfunction associated with the *fluid perturbation W*. The normalization of Fig. 7 is preserved here, and we find that the f-mode (filled symbols) has an order-of-magnitude larger amplitude than the w-mode (open symbols). This is further evidence of the different natures of the two kinds of modes: w-modes are primarily gravitational-wave modes, while f-modes are primarily fluid modes.

coupling between the strings was the same for all modes. In our case, the coupling is a gravitational one, and it is a commonplace observation that short-wavelength gravitational perturbations do not couple so strongly to the fluid as long-wavelength ones: for example, the Cowling approximation is very good for higher order p- and g-modes. If this holds for the w-modes, then one would expect a slow increase in the imaginary part of the frequency as one goes along the sequence.

(ii) The size of the imaginary part of the frequency in the toy problem was smaller than or comparable to that of the lowest order real part when the dimensionless coupling constant was greater than about 0.01. If this coupling corresponds in the stellar case to something like M/R, then the relative sizes of the real and imaginary parts of the frequencies are similar in the two problems.

(iii) Perhaps most convincingly, the fluid part of the eigenfunctions of the modes (the function W) is very weak compared to its typical value for f-modes.

We conclude from this that the strongly damped modes of the star, which we have christened w-modes, do in fact exist.

Despite their quick damping, these modes are more than mere curiosities. In the first milliseconds after the formation of a neutron star in collapse, the radiation that comes out will be due to two sources. The first is the obvious one, namely the fluid motions during collapse; but the second will be whatever initial gravitational-wave data the collapse itself generates. The w-modes may well be strongly in evidence within the burst of gravitational waves that follows gravitational collapse. Their signature, of a ringing with damping on a few cycles, would be very similar to the signature found by Sun & Price (1988) for the normal modes of black holes formed in gravitational collapse, and would be very different from the very slowly decaying but much smaller amplitude ringing of the p-modes. In fact, techniques similar to those used by Sun & Price could be applied here to predict how much excitation the w-modes will suffer as a result of a collapse.

Moreover, the w-modes are likely to be essential in any proof that the normal modes of a relativistic star are complete for some sort of initial data. A completeness proof of this type is one of the principal unsolved problems of relativistic stellar perturbation theory, and was one of the motivations of the Sun & Price work on black holes.

It is also conceivable that in more complex situations, such as stars with rotation or especially stars with ergoregions, the w-modes could (like the f-modes) become unstable, and thereby place a limit on the rotation rate of stars. But we feel that it is unlikely that this limit will be stronger than that provided by effects already known, such as the f-mode instability (Chandrasekhar 1970; Friedman & Schutz 1978).

In addition, the w-modes may prove to be *prototypes* for other families of modes that arise in relativistic stars. The essential features of the present problem are, we feel, as follows. A new or hitherto neglected effect (in this case, general relativity) couples two very different systems: one in which there is a well-defined spectrum of normal modes (the Newtonian star with its f-, p- and g-modes) and the other a wave system on an infinite domain in which there are no conventional modes at all, because in the absence of coupling it has no means of trapping or reflecting waves (here, the gravitational-wave field of Minkowski space-time). The coupling results in two distinct families of modes: the first is (for weak coupling) a small change in the already-established family (f-modes of relativistic stars acquire a small damping), while the other is a completely new spectrum of strongly damped modes, whose damping *increases* as the coupling increases (the w-modes here).

Another relativistic system that may show similar spectral effects is the problem recently introduced by Chandrasekhar & Ferrari (1991b). In non-rotating relativistic stars, the so-called even-parity perturbations give rise to the f-, p- and g-modes that we have referred to here. But there are also odd-parity perturbations in both the fluid and the gravitational-wave field that do not, however, couple to each other or to the even-parity perturbations. Chandrasekhar & Ferrari study what happens when the star has a small amount of rotation: the non-sphericity of the resulting metric couples the even- and odd-parity perturbations together.

The Chandrasekhar–Ferrari problem resembles the *w*-mode problem in that the coupling brings together an established spectrum (the even-parity modes) with a wave field (the odd-parity gravitational perturbations). This should give rise to some modes with strong damping. This problem is complicated, however, by the coupling of an additional odd-parity system, the fluid perturbations, that have a well-defined spectrum, albeit completely degenerate at zero frequency in the absence of coupling. From these may arise in addition a weakly damped spectrum in which the imaginary part of the frequency is of the same order as the real part, both going to zero as the coupling decreases. This fascinating problem will surely merit further study, not only because of its intrinsic interest but also because, as Chandrasekhar & Ferrari point out, the new modes may provide observable evidence of the Lense–Thirring effect ('dragging of inertial frames'), which has so far not been directly observed in any physical system.

The *w*-modes represent, therefore, not only the completion of the spectrum of normal modes of a non-rotating star in general relativity, but also a new class of mode that may have important physical ramifications and that we may expect to see in other situations where finite systems like stars are coupled to radiative fields. In this paper we have firmly established their existence, reassured ourselves of the reliability of our earlier toy model (Kokkotas & Schutz 1986), and confirmed some of the earlier numerical results of Kojima (1988). Probably the most important impediment to learning more about them is the lack of a numerical method that can handle the exponential behaviour of the modes at infinity. The application of improved methods of numerical integration would open the way to studying the dependence of these modes on the structure of the star (especially in more realistic stars), and the origin and reality of the curious kinks in the spectrum seen in each model. It would also be interesting to study the relationship of these modes to those of black holes, and to see if they can be made to go unstable in any situations.

ACKNOWLEDGMENTS

KDK acknowledges the Department of Physics and Astronomy of the University of Wales College of Cardiff for its hospitality and SERC for its financial assistance.

REFERENCES

Balbinski, E., Detweiler, S., Lindblom, L. & Schutz, B. F., 1985. *Mon. Not. R. astr. Soc.*, **213**, 553.
Chandrasekhar, S., 1970. *Phys. Rev. Lett.*, **24**, 611.
Chandrasekhar, S. & Detweiler, S., 1975. *Proc. R. Soc. London A*, **344**, 441.
Chandrasekhar, S. & Ferrari, V., 1991a. *Proc. R. Soc. London A*, **432**, 247.
Chandrasekhar, S. & Ferrari, V., 1991b. *Proc. R. Soc. London A*, **433**, 423.
Detweiler, S. & Lindblom, L., 1985. *Astrophys. J.*, **292**, 12.
Fackerell, E. D., 1971. *Astrophys. J.*, **166**, 197.
Friedman, J. L. & Schutz, B. F., 1978. *Astrophys. J.*, **222**, 281.
Guinn, J. W., Will, C. M., Kojima, Y. & Schutz, B. F., 1990. *Class. Quant. Grav.*, **7**, L47.
Kojima, Y., 1988. *Prog. theor. Phys.*, **79**, 665.
Kokkotas, K. D., 1985. *MSc thesis*, University of Wales.
Kokkotas, K. D. & Schutz, B. F., 1986. *Gen. Rel. Grav.*, **18**, 913.
Lindblom, L. & Detweiler, S., 1983. *Astrophys. J. Suppl.*, **53**, 73.
Press, H. W., Flannery, B. P., Teukolsky, S. A. & Vetterling, T. W., 1986. *Numerical Recipes: The Art of Scientific Computing*, Cambridge University Press, Cambridge.
Schutz, B. F., 1983. *A First Course in General Relativity*, Cambridge University Press, Cambridge.
Schutz, B. F., 1989. *Class. Quant. Grav.*, **6**, 1761.
Schutz, B. F. & Will, C. M., 1985. *Astrophys. J. Lett.*, **291**, L33.
Sun, Y. & Price, R. H., 1988. *Phys. Rev. D*, **38**, 1040.
Thorne, K. S. & Campolattaro, A., 1967a. *Astrophys. J.*, **149**, 591.
Thorne, K. S. & Campolattaro, A., 1967b. *Astrophys. J.*, **152**, 673.
Zerilli, F. J., 1970. *Phys. Rev. Lett.*, **24**, 737.